1521-0103/361/1/115–121$25.00
THE JOURNAL OF PHARMACOLOGY AND EXPERIMENTAL THERAPEUTICS

http://dx.doi.org/10.1124/jpet.116.239509
J Pharmacol Exp Ther 361:115–121, April 2017

The Journal of PHARMACOLOGY And Experimental Therapeutics

Therapeutic Restoration of Endothelial Glycocalyx in Sepsis

J.W. Song, J.A. Zullo, D. Liveris, M. Dragovich, X.F. Zhang, and M.S. Goligorsky

Renal Research Institute and Departments of Medicine, Pharmacology and Physiology (J.A.Z., M.S.G.), and Department of Microbiology (D.L.), New York Medical College, Valhalla, New York; Department of Anesthesiology and Pain Medicine, Yonsei University College of Medicine, Seoul, South Korea (J.W.S.); and Department of Mechanical Engineering and Mechanics, and Bioengineering Program, Lehigh University, Bethlehem, Pennsylvania (M.D., X.F.Z.)

Received December 12, 2016; accepted February 2, 2017

ABSTRACT

Endothelial glycocalyx (EG) is disintegrated during sepsis. We have previously shown that this occurs very early in the course of sepsis and its prevention improves the survival of mice with sepsis. Here, we sought to investigate the possibility of pharmacologically accelerating the restoration of disintegrated EG in sepsis. We used a soilage injection model to induce polymicrobial sepsis in C57/BL6 mice and measured total body EG. En face aortic preparations were used for staining of markers of EG and atomic force microscopy was used to measure EG in vitro. In vitro studies were conducted in cultured endothelial cells either exposed to a lipopolysaccharide or enzymatically denuded of EG. Sulodexide (SDX), a heparin sulfate-like compound resistant to degradation by heparanase, accelerated EG regeneration in vitro and in vivo. The total volume of EG was drastically reduced in septic mice. Administration of SDX produced a dramatic acceleration of EG restoration. This effect, unrelated to any SDX-induced differences in microbial burden, was associated with better control of vascular permeability. Notably, SDX demonstrated not only a remarkable capacity for EG regeneration in vitro and in vivo but was also associated with improved animal survival, even when instituted 2 hours after induction of severe sepsis. In conclusion, 1) EG is disintegrated in sepsis, the event which contributes to high animal mortality; 2) pharmacologic acceleration of EG restoration can be achieved using SDX; and 3) SDX reduces vascular permeability, which is elevated in septic mice, and improves animal survival.

Introduction

Sepsis is defined as a systemic inflammatory syndrome induced by bacterial infection that can lead to multiorgan failure. It afflicts more than 750,000 people annually in the United States alone and has mortality rates of 28%–50%. One of the key molecular causes of gram-negative septicemia is endotoxin consisting of lipopolysaccharides (LPS) bound with high affinity to LPS-binding glycoprotein that is recognized by TLR4 and co-receptor CD14 on monocytes/macrophages and endothelial cells (Aird, 2003). Considering the systemic nature of septicemia, vascular endothelium represents the first line of exposure to bacterial endotoxins (Morrison and Ulevitch, 1978). It responds to endotoxins with a complex system of danger signals, which are chronologically sequenced and spatially propagated (Ratliff et al., 2013). Functionally, these waves of danger signaling tend to secure proper organismal responses, both pro- and anti-inflammatory.

Endothelial glycocalyx (EG) represents a surface layer consisting of glycoproteins, proteoglycans, and glycosaminoglycans. Due to its unique location, this structure provides a passive barrier to water and solute transport, the interaction between circulating cells and the endothelial cells forming the inner wall of blood vessels, and serves as a sensor of mechanical forces, such as shear stress and pressure, and represents a shielding instrument for cell surface receptors preventing their hyperactivation (Reitsma et al., 2007; Becker et al., 2010a). However, this structure is quite vulnerable and tends to disintegrate after application of various stressors, such as endotoxins, ischemia/hypoxia/reperfusion, oxidative stress, among others. Damage to and modification of the EG are observed in many diseases including diabetes, ischemia, chronic infectious diseases, atherosclerosis, and tumors (van den Berg et al., 2003; Reitsma et al., 2007; Weinbaum et al., 2007; Becker et al., 2010b; VanTeeffelen et al., 2010; Chappell et al., 2011). The disintegration of EG predisposes to tissue infiltration by polymorphonuclears, monocyte/macrophages, and lymphocytes. It also leads to hyperactivation of plasma membrane receptors by unhindered exposure to ligands and further activation of danger signaling. EG has a high rate of turnover: for instance, one of its components, hyaluronan, is synthesized at a rate of 5 g/d and one-third of its 15 g pool is degraded daily (Fraser et al., 1997).

These studies were supported by the National Institutes of Health [Grants DK54602, DK052783, and DK45462 (to M.S.G.)]; New York Trust Fund (to M.S.G.); the ILJIN Faculty Research Assistance Program of Yonsei University College of Medicine for 2013 [Grant 6-2013-0068] (to J.W.S.); and the Basic Science Research Program through the National Research Foundation of Korea (NRF) funded by the Ministry of Science, ICT & Future Planning [Grant NRF-2013R1A1A1010863] (to J.W.S.).
dx.doi.org/10.1124/jpet.116.239509.

ABBREVIATIONS: AFM, atomic force microscopy; DAPI, 4′,6′-diamidine-2′-phenylindole dihydrochloride; EG, endothelial glycocalyx; FIP, feces-induced peritonitis; FITC, fluorescein isothiocyanate; HS, heparan sulfate; LPS, lipopolysaccharide; MMP, matrix metalloproteinase; PBS, phosphate-buffered saline; SDX, sulodexide; WGA, wheat germ agglutinin.

We have recently demonstrated that the loss of EG represents a very early event in the pathogenesis of sepsis (Zullo et al., 2016). It is linked to exocytosis of lysosome-related organelles and degradation of glycocalyx. Suppression of the exocytosis of these organelles resulted in improved preservation of glycocalyx and better survival of animals. However, in the clinical practice physicians are confronted with on-going sepsis when glycocalyx is by and large destroyed. Therefore, clinically a more rationale strategy would be related to acceleration of the restoration of EG. The present study summarizes our attempts to achieve this goal. Specifically, one of the authors (Zullo, 2016) screened the effects of heparin sulfate, high molecular weight hyaluronic acid, an inhibitor of hyaluronidase (Hyaluromycin), and a heparanase inhibitor, OGT 2115, individually and in combination, on the rate of glycocalyx restoration following its degradation. A combination therapy of cultured endothelial cells proved to be most effective. Similar efficacy was noted using sulodexide (SDX) (Vessel, Alfa Wassermann, Milan, Italy, PubChem CID: 14366984), a highly purified patented technology extraction product from porcine intestinal mucosa that consists of 80% iduronylglycosaminoglycan sulfate (known as fast-moving heparin) and 20% dermatan sulfate. SDX is a pluripotent compound: it has been shown to possess heparanase-inhibitory activity; the ability to restore EG in diabetes; inhibit matrix metalloproteinase (MMP) release from leukocytes; inhibit IL-6 and other cytokines; stimulate lipoprotein lipase activity; and suppress coagulation and stimulation of fibrinolysis (Masola et al., 2012; Hoppensteadt and Fareed, 2014). For these reasons, we have focused the present study on the role of this compound in facilitating the regeneration of glycocalyx. In vitro and in vivo findings support the efficacy of SDX in improved restoration of glycocalyx, amelioration of increased vascular permeability, and improved survival of mice with severe sepsis.

Materials and Methods

Cell Culture. The bEnd.3 immortalized mouse brain microvascular endothelial cells were used (American Type Culture Collection (Manassas, VA). Cells were cultured in Dulbecco's modified Eagle's medium with supplemental 10% fetal bovine serum, 1% penicillin, and 50 μg/ml streptomycin, and atmosphere of 5% CO_2 at 37°C.

Animal Models of Sepsis. All animal experiments were performed in accordance with National Institutes of Health Guide for the Care and Use of Laboratory Animals and approval by the Institutional Animal Care and Use Committee. We used C57/BL6 male mice between 10 and 11 weeks of age. Sepsis was induced by one of the following methods: 1) intraperitoneal injection of LPS (10 mg/kg) or 2) fecal pellets suspended in phosphate-buffered saline (PBS) [i.e., the feces-induced peritonitis (FIP) model].

For the FIP model, fecal pellets were collected from the animal cages and suspended in PBS at a ratio of 120 mg pellet per 1 ml PBS. The suspension was filtered through a 100 μm nylon mesh cell strainer and stored with 15% glycerol at −80°C until injection. For survival experiments and bacterial cultures, 200 μl of fecal suspension per mouse was injected intraperitoneally. For measurements of glycocalyx and vascular permeability, 100 μl per mouse was injected 16 hours before the measurements. Animals received SDX (kindly supplied by Alfa-Wassermann, Milan, Italy) or equal volume of PBS subcutaneously 2 hours after the induction of sepsis.

Animal Survival. Mice subjected to FIP were kept under continuous video surveillance for 5 days (120 hours) and housed in their native habitats throughout the time period to minimize new environmental stressors. Light and dark cycles were kept constant and in accordance with the Institutional Animal Care and Use Committee protocols. Death was the principle endpoint. Mice living beyond the observation period of 5 days were euthanized in accordance with the Institutional Animal Care and Use Committee protocols to minimize any potential for undue suffering.

Bacterial Culture. The blood and peritoneal lavage samples were obtained 16 hours after FIP. The peritoneal cavity was washed with 1 ml of PBS and the blood samples were collected from the left ventricle. The samples were serially diluted in tryptic soy broth and 100 μl of each diluted sample was spread on a tryptic soy agar (tryptic soy broth) plate. The culture plates were incubated in an anaerobic jar at 37°C for 24 hours and the number of colonies/dish was counted.

Measurements of EG In Vitro. The bEND.3 cells were cultured in a 48-well cell culture plate until confluent. The cell monolayers were fixed with 1:1 mixture of acetone and methanol at −20°C for 20 minutes, followed by 1 hour incubation with 20 μg/ml fluorescein isothiocyanate (FITC)–conjugated wheat germ agglutinin (WGA) lectin (Sigma-Aldrich, St Louis, MO) in 5% bovine serum albumin at 4°C. After careful washing with PBS, fluorescence intensity was measured at excitation/emission wavelengths of 485/540 nm by a Biotek synergyHT microplate reader (Biotek, Winooski, VT) or images were obtained using an upright Nikon Y-FL epifluorescence microscope (Nikon Inc., Melville, NY) at 600× magnification.

An established atomic force microscopy (AFM) nanoindentation assay (Oberleithner et al., 2011; Wiesinger et al., 2013; Dragovich et al., 2016) was conducted to determine the thickness of the glycocalyx. All single-molecule force measurements were conducted using a custom-designed AFM that employs a single-axis piezoelectric translator equipped with a strain gauge (Physik Instrumente, Waldbronn, Germany) to control the absolute position of the AFM cantilever (Kusche-Vihrog and Oberleithner, 2012; Dragovich et al., 2016). The deflection of the cantilever was monitored optically using an inverted optical system attached to the AFM. The detection limit of this AFM was in the range of 10 pN. The AFM probes used in this study were MLCT-BIO nitride levers (Bruker AFM Probes, Camarillo, CA). The spring constant at the tip was calibrated via thermally induced fluctuations.

Total Volume of EG. The comparative analysis of the volume of distribution (V_d) of glycocalyx-penetrating (40 kDa dextran) and non-penetrating size-excluded tracers (70 and 500 kDa dextran) was developed by Nieuwdorp et al. (2006a,b) and modified by us. Briefly, a total of 100 μl of fluorescent-labeled dextran solution [3.75 mg/ml of 40 kDa dextran-Texas red and 3.75 mg/ml of 70 kDa dextran-FITC (in the initial experiments); 500 kDa dextran-FITC in 1% albumin-PBS solution (in subsequent experiments)] was injected into the left jugular vein of C57BL/6 male anesthetized mice 16 hours after the induction of sepsis (FIP, LPS) or equal volume of intraperitoneal PBS injection (control). Regular 50 μl blood samples were drawn from the right jugular vein at 3, 5, 10, and 15 minutes. The heparinized blood samples were then immediately centrifuged (10 minutes at 3000 rpm) and 20 μl plasma was collected and stored at −20°C until further analysis. The plasma samples were diluted to 1:10 in PBS in a 96-well plate. The fluorescence intensity was measured at 575/620 nm for the 40 kDa dextran-Texas red and 485/540 nm for the 70 or 500 kDa dextran-FITC. The concentrations of both dextrans in each sample were calculated from linear least-squares fitting determined by fluorescence measurement of serially diluted dextran solution in PBS. The concentration (C)/time (t) curve for each dextran was constructed and fitted with a least-squares monoexponential function ($C = C_0e^{-\lambda t}$). The initial volume of distribution for each dextran was calculated from the total amount of injected dextran (0.375 mg) divided by the concentration at time zero (C_0). The difference between the initial volume of distribution for each dextran represents the whole body glycocalyx volume ($V_{\text{glycocalyx}} = 0.375/C_1e^{-\lambda 1t} - 0.375/C_2e^{-\lambda 2t}$; where $t = 0$). To illustrate with an example, ideal calculations approximate the 40 kDa monoexponential curve to be approximately $C_{40\text{ kDa}} = 0.48e^{-0.03t}$, and ideal calculations approximate the 70 kDa curve to be $C_{70\text{ kDa}} = 0.52e^{-0.01t}$. The initial V_d values at $t = 0$ were 0.78 ml (0.375/0.48) and 0.72 ml (0.375/0.52) for

40 and 70 kDa dextran, respectively. Subtracting the V_d value at 70 kDa from the V_d value at 40 kDa reveals the glycocalyx volume of distribution to be 0.06 ml (60 μm^3). In preliminary experiments we ruled out the possibility of artifacts due to the emission of cross-reading from two fluorophores and interference of heparin present in the samples with fluorescence detection (data not shown).

Immunofluorescence Staining of En Face Aorta. Mice were anesthetized with isoflurane. The heart and abdominal portion of the posterior vena cava was exposed. Immediately after cutting the posterior vena cava, the left ventricle was punctured from the apex and perfused with 10 ml of 2 mM EDTA in PBS over 20 minutes, followed by perfusion-fixation with a 5 ml of 1:1 mixture of acetone/methanol at −20°C. The washout of blood was confirmed by observing clear perfusate from the posterior vena cava. The descending thoracic aorta was exposed. After a longitudinal incision to expose a luminal surface, the aorta was carefully excised and stored in 1:1 mixture of acetone/methanol at −80°C until analysis. The en face preparation of aorta was stained with 20 μg/ml WGA lectin-FITC for 1 hour at room temperature, or antibodies against heparan sulfate (HS) or syndecan-4. For HS and syndecan-4 staining, the aorta preparation was incubated with anti-HS rat monoclonal primary antibody (1:200 dilution; Abcam, Cambridge, MA) and anti-syndecan 4 mouse monoclonal primary antibody (1:200 dilution; Santa Cruz Biotechnology, Santa Cruz, CA) overnight at 4°C, followed by washing with PBS and an incubation with Alexa Fluor 488-conjugated secondary antibody (for anti-HS, 1:500 dilution; Thermo Fischer Scientific, New York, NY) and phycoerythrin-conjugated secondary antibody (for syndecan-4, 1:500 dilution; Santa Cruz Biotechnology) for 2 hours at room temperature.

Measurement of Vascular Permeability. Vascular permeability was measured in lungs and peritoneum at 16 hours after the induction of sepsis (FIP) or equal volume of intraperitoneal PBS injection (control) according to the previously described protocol (Vlasenko and Melendez, 2005; Ghosh et al., 2012). Briefly, 100 μl of 1% Evans blue was injected via jugular vein 1 hour before the termination of the experiment (15 hours after the induction of sepsis) to assess extravasation of Evans blue. To assess lung vascular permeability, the right ventricle was punctured and perfused with 10 ml of 2 mM EDTA in PBS over 20 minutes. The perfusate was drained via the opened posterior vena cava. The lungs were excised and homogenized in formamide (1 ml/100 μg tissue), and then incubated for 16 hours at 60°C. To assess the leakage of Evans blue into the peritoneal cavity, 1 ml of PBS was injected and aspirated to wash the peritoneal cavity. The homogenized lungs and peritoneal lavage samples were centrifuged at 5000*g* for 30 minutes, and the optical density of the supernatant was measured by a spectrophotometer at 620 and 740 nm. The contamination of samples with heme pigments was corrected using the following equation: $E620_{corrected} = E620_{raw} - (1.426 \times E740_{raw} + 0.030)$.

Statistical Analyses. Data are expressed as mean ± S.E.M., unless otherwise mentioned. Data were analyzed using an independent *t* test or one-way analysis of variance. The *P* values for multiple comparisons were adjusted by the Tukey-Kramer's procedure. Survival data were analyzed by the log-rank test. All statistical analyses were performed with NCSS 11 (NCSS Statistical Software, Kaysville, UT) and *P* values less than 0.05 were considered as statistically significant.

Results

In Vitro Experiments. Endothelial cells were treated with LPS for 1 hour followed by SDX or a vehicle for 8 hours. Cells were fixed in acetone/methanol, stained with FITC-WGA-lectin, washed with PBS, and fluorescence intensity was detected using a fluorescence plate reader. LPS resulted in a significant drop of FITC-WGA-lectin fluorescence, consistent with disintegration of EG. However, delayed treatment with SDX (20 μg/ml) restored EG (Fig. 1).

We next used an entirely different, fluoroprobes-unrelated technical approach and another model of denuding glycocalyx, namely, treatment of endothelial cells with heparanase and hyaluronidase. In these experiments using AFM we reexamined these findings. An AFM indentation assay was conducted to determine the thickness of the glycocalyx (Fig. 2). During the indentation scan, the AFM tip travels vertically toward the surface of an endothelial cell. Upon indentation of the EG, the AFM cantilever, serving as a soft spring, is deflected (Fig. 2A). The deflection of the cantilever is measured and plotted as a function of the sample position along the *z* axis. The resulting curve is transformed into a force-versus-indentation curve using the cantilever's spring constant and the light lever sensitivity. The slope of the force-indentation curve directly reflects the stiffness (expressed in pN/nm), which is necessary to indent the EG for a certain distance. The first slope indicates the stiffness (in this tracing, 0.07 pN/nm) of the very first layer, which is the EG. The second nonlinear region indicates the stiffness of the cortical membrane. The distance between the starting point of the EG indentation and the starting point of the second slope (projected on the *x* axis) corresponds to the thickness of the EG. On average, the glycocalyx thickness was found to be 0.58 ± 0.07 μm before removal by heparanase I and III and hyaluronidase. After treatment of the bEnd.3 endothelial cells with 25 mU/ml heparanase I and III and 20 μg/ml hyaluronidase, the soft, linear glycocalyx indentation region had disappeared. After 12 hours of recovery, the AFM was still unable to detect the presence of the EG. In contrast, when 20 μg/ml of SDX was added to the cells at 2 hours after enzymatic degradation, glycocalyx was fully restored after 10 hours of incubation (0.54 ± 0.05 μm).

In Vivo Experiments. Based on the aforementioned findings the focus of the study was shifted exclusively to investigation of SDX effects in vivo. For these studies, after exhaustive search for the most appropriate model of sepsis, we elected the soilage model of polymicrobial sepsis, as detailed in *Materials and Methods*. The reasons for this choice were 1) the self-reparatory nature of LPS model and 2) the fulminant course of the cecal ligation-puncture model. In either case, the time course was not amenable to the conduct of the studies presented subsequently.

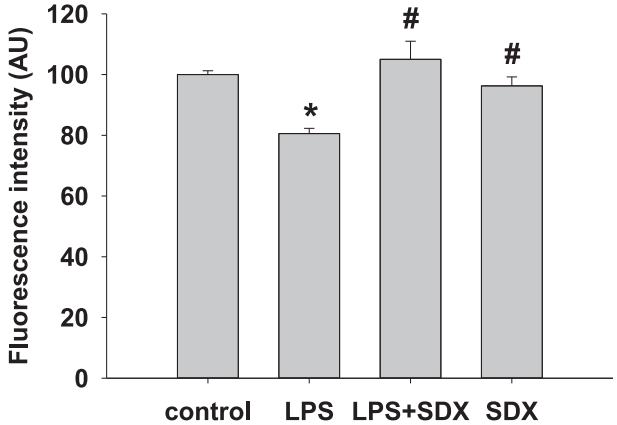

Fig. 1. Effect of SDX and LPS on the glycocalyx of bEnd3 cells. Cells were cultured to 90% confluency and treated with SDX alone for 8 hours, LPS for 1 hour, or 1 hour of LPS followed by SDX for 8 hours. Cells were fixed in acetone/methanol, stained with FITC-WGA-lectin for 1 hour, washed with PBS and immediately read on a fluorescent plate reader. Data are represented as mean ± S.E.M. ($n = 6$). *$P < 0.05$ versus control; #$P < 0.05$ versus LPS.

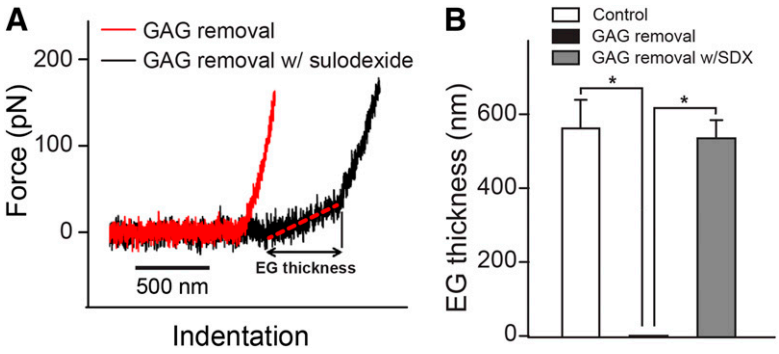

Fig. 2. Effect of SDX on restoration of EG after enzymatic removal measured by AFM. (A) Typical AFM indentation traces of a bEnd.3 cell at 12 hours post glycosaminoglycan (GAG) removal (red) and a cell treated with SDX (20 μg/ml) 2–12 hours after enzymatic removal of glycocalyx. (B) EG thicknesses of control, GAG removal, and GAG removal with SDX treatment groups. Data are represented as mean ± S.E.M. ($n > 10$). *$P < 0.05$ between indicated groups.

First, we examined the end effect of SDX therapy of polymicrobial sepsis. The dose-response curve of SDX-treated septic mice on their survival rate is presented by Kaplan-Meyer curves (Fig. 3). Notably, lower doses of SDX exerted little effect on animal survival; however, 40 mg/kg resulted in remarkable improvement in survival rates of septic mice receiving 40 mg/kg of SDX (hazard ratio, 0.11 95%; confidence interval, 0.02–0.59; $P = 0.015$). Therefore, this relatively high dose was used in the subsequent experiments. Based on the available data on the pharmacokinetics of SDX in humans (Coccheri and Mannello, 2014), the dose used should be sufficient for the duration of the experiments (16 hours after induction of sepsis and 14 hours after SDX administration)

To rule out any possible effects of SDX treatment on the bacterial burden, we next performed anaerobic bacterial cultures of blood and peritoneal lavage fluid obtained from mice at 16 hours after induction of sepsis. As shown in Fig. 4, SDX treatment did not affect the microbial burden, thus we rejected this mechanism as being responsible for the observed improvement in survival of septic mice.

In view of the profound effects of sepsis on vascular permeability, we next examined the consequences of SDX injection to septic mice on this parameter. Both the lung and peritoneal permeability were measured using spectrophotometric detection of intravenously injected Evans blue. As shown in Fig. 5, A and B, retention of Evans blue in lungs and peritoneal fluid was increased, indicative of vascular permeability being dramatically elevated in septic animals. SDX treatment significantly mitigated the sepsis-induced increase in vascular permeability.

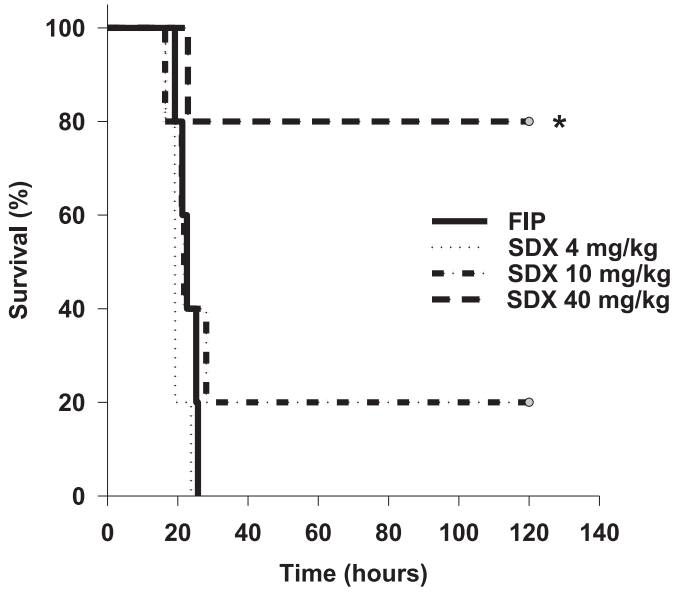

Fig. 3. Effect of treatments on septic mortality in mice. Kaplan-Meyer survival curves in mice with polymicrobial sepsis treated with vehicle or different doses of SDX were constructed.

Since EG is critical for maintenance of vascular permeability, we next examined the effects of SDX on the integrity of this structure. To understand the regenerative capacity of the glycocalyx and the effects of SDX in vivo, we set out to establish a reliable, minimally invasive whole body glycocalyx assay. An indicator dilution of FITC/500 kDa dextran (non-penetrating glycocalyx) and Texas-red/40 kDa dextran (glycocalyx penetrating) were simultaneously injected intravenously. Blood samples were taken at set intervals and read on a spectrofluorometer for fluorescent intensity. The 40 and 500 kDa dextrans measure whole body glycocalyx volume based on their differential volume of distribution: 40 kDa dextran can percolate through the EG; however, 500 kDa dextran is size-excluded from the glycocalyx and can only occupy a luminal volume. Taken together, the difference in volume of distribution of the dextrans indirectly measures the volume of the glycocalyx, as shown in Fig. 6A. The similarity of slopes for concentration of 40 kDa between control and sepsis suggests that the pharmacokinetic property of 40 kDa dextran was not significantly altered by sepsis; in intact mice the total volume of EG equaled approximately 54 ± 8 μl. The indicator dilution technique was used to investigate glycocalyx changes during soilage-induced polymicrobial sepsis and to follow the capacity of the glycocalyx to regenerate. In these experiments we used injection of fecal suspension to overcome high mortality rates in untreated animals. Figure 6B depicts the results of total glycocalyx volume measurements in septic mice with or without SDX treatment. The data show that treatment with SDX instituted 2 hours after induction of sepsis resulted in a dramatic restoration of total body glycocalyx 16 hours later. Similar data were obtained using the LPS model of sepsis: a delayed injection of SDX significantly improved the integrity of EG (Fig. 6C).

Studies of aortic EG were performed using detection of individual components, such as WGA-lectin binding, HS, and syndecan 4. As shown in Fig. 7, all three markers of the glycocalyx were significantly depleted in septic mice. SDX treatment of these animals resulted in the tendency toward restoration of staining patterns and intensity. Staining of en face aortas with WGA-lectin showed a statistically significant restoration of EG within the selected timeframe (Fig. 7A).

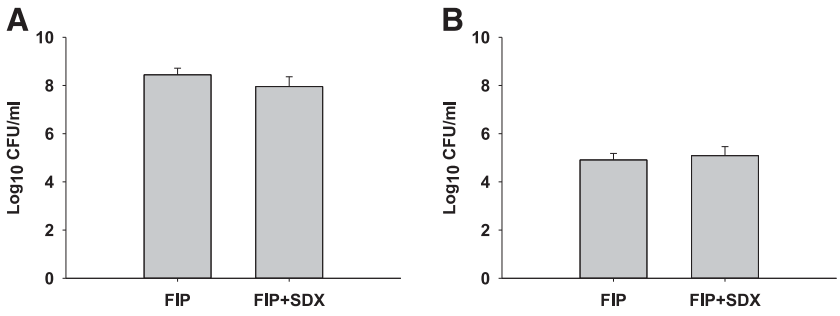

Fig. 4. Effect of treatments on peritoneal and circulatory bacteria. Peritoneal lavage (A) and blood (B) samples were taken 16 hours after induction of sepsis and cultured anaerobically for 24 hours. Data are represented as mean ± S.E.M. (n = 6).

We next inquired whether neutrophil glycocalyx was similarly degraded in severe sepsis, and if that occurs could SDX therapy restore it as efficiently. Blood smears were stained with WGA and costained with DAPI (4′,6′-diamidine-2′-phenylindole dihydrochloride) (for identification of neutrophils). As demonstrated in Fig. 8, severe polymicrobial sepsis was associated with the loss of glycocalyx integrity in neutrophils and the restoration of glycocalyx was facilitated by SDX treatment.

Discussion

The data presented herein show that acceleration of restoration of EG in activated stressed endothelial cells in culture and in septic mice is achievable with the use of a single compound that possesses multifaceted actions (SDX). There are sparse and conflicting data on pharmacological restoration of glycocalyx. On the one hand, blockade or knockout of CD44, a major receptor for hyaluronan, reduced IL-2-induced vascular leak (Guan et al., 2007), thus arguing that disintegration of EG is beneficial in preserving vascular permeability. This is sharply contrasted by several studies that demonstrated the opposite—restoration or preservation of EG components is beneficial in sepsis and for preserving vascular permeability (Lipowsky et al., 2011; Spicer and Calfee, 2012).

The earliest attempts to restore glycocalyx were recorded by Henry and Duling (1999), who infused the combination of hyaluronan and chondroitin sulfate. Other investigators followed the use of these compounds or syndecan-1 (Kaneider et al., 2003; Potter and Damiano, 2008; Becker et al., 2010a) and confirmed the previous conclusions. Attempts to inhibit sheddases responsible for degradation of EG have been presented (Becker et al., 2015). Among successful attempts to inhibit glycocalyx degradation was the use of the MMP inhibitor doxycycline (Lipowsky et al., 2011). Compared with the aforementioned therapeutic compounds, SDX not only contains fast-moving heparin and dermatan sulfate but also exerts antiheparanase and MMP-inhibitory activity (Masola et al., 2012; Hoppensteadt and Fareed, 2014).

It has been demonstrated that complete restitution of HS after its enzymatic degradation requires 12 hours (Giantsos-Adams et al., 2013). It has previously been determined that after degradation of EG with either hyaluronidase, heparanase III, or TNF-α the restoration of hydrodynamically relevant glycocalyx in vivo requires ~7 days (Evanko et al., 2007). Attempts to accelerate restoration of EG have been entertained. It is not excluded that providing hyaluronan of appropriate size may by itself facilitate restoration of EG (Jiang et al., 2007; Zhang et al., 2008). In our preliminary experiments, we examined a list of pharmaceuticals theoretically capable of restoring the integrity of EG. It turned out that SDX contains not only fast-moving heparin and dermatan sulfate but also exerts heparanase- and MMP-inhibitory activity. The fast-moving heparin component is responsible for the heparanase inhibition by SDX. As a closest mimic of HS, heparin inhibits the binding and recognition of HS at basic clusters of heparanase in a competitive manner (Vlodavsky et al., 2007). The dermatan sulfate fraction of SDX is thought to inhibit MMP-9 by interaction with the active zinc binding site of the pro-MMP-9 molecule, preventing its conformational change to an active form (Mannello and Raffetto, 2011). SDX also reduces the release of MMP-9 from leukocytes (Mannello et al., 2013). No study has specifically investigated whether SDX inhibits these enzymes irreversibly; however, it has a favorable pharmacokinetic profile with a long half-life of 19–25 hours. All of these properties indicate SDX has the potential to facilitate glycocalyx restoration.

As shown previously, SDX-induced improved survival of mice with the soil model of sepsis is not attributable to any detectable changes in the microbial burden. This conclusion is further supported by the finding that SDX has a beneficiary effect in the LPS-induced model of sepsis, which bypasses micro-organismal installation. On the other hand, a significant increase in sepsis-related vascular permeability (Chelazzi et al., 2015) is curtailed by SDX. Although SDX is credited with anti-inflammatory and antithrombotic actions (Hoppensteadt and Fareed, 2014), it is likely that correction of vascular permeability is related to the

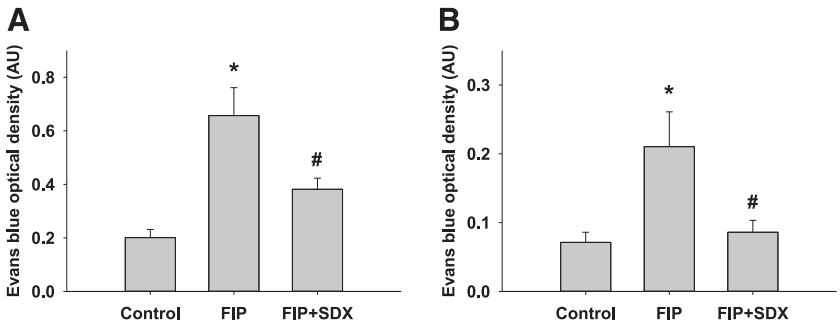

Fig. 5. Evans blue determination of vascular permeability of the peritoneal (A) and pulmonary vessels (B) in mice with polymicrobial sepsis. Data are represented as mean ± S.E.M. (n = 6). *P < 0.05 versus control; #P < 0.05 versus FIP.

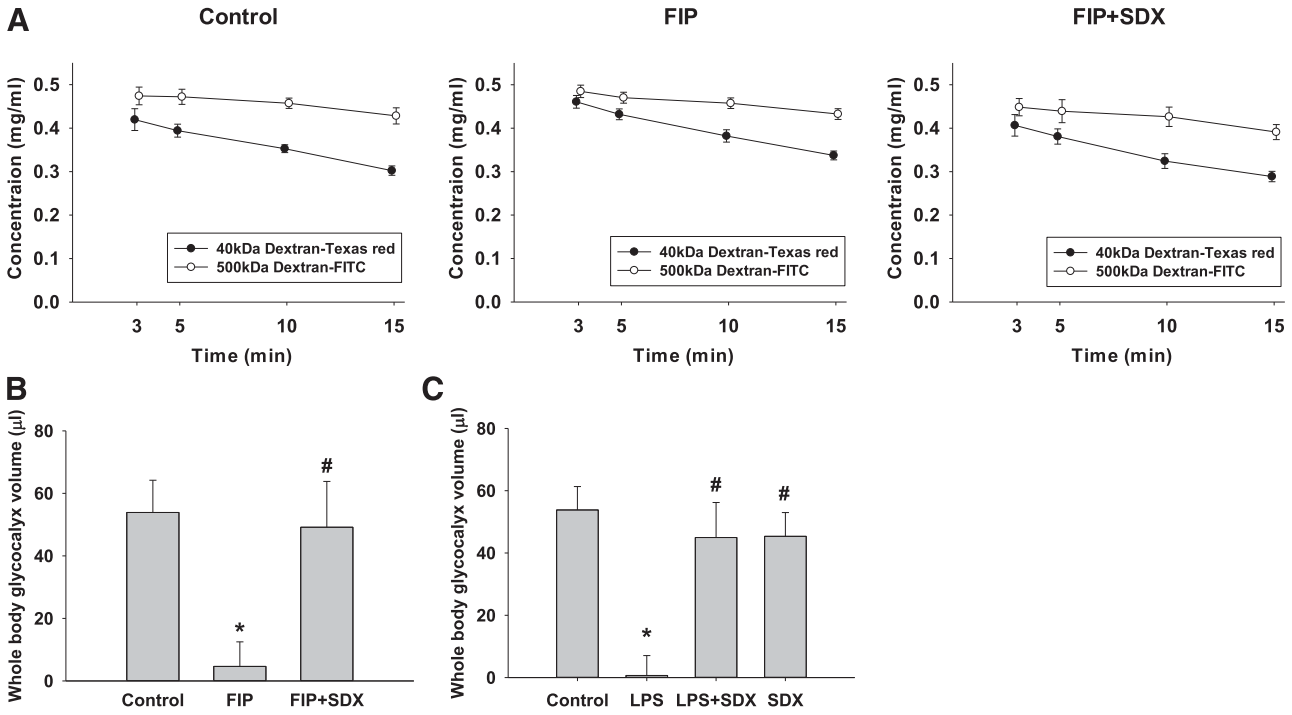

Fig. 6. EG volume in control and septic mice. Volume was determined by the difference in the volume of distribution between 40 and 500 kDa dextran. (A) Dilution curves for each fluorophore in control and SDX-treated or untreated FIP. (B) Diagram of the in vivo whole body EG in the FIP model of sepsis. (C). In vivo glycocalyx volume of distribution measurements in LPS mice receiving therapy with SDX. Utilizing a whole body glycocalyx measurement through a dextran size exclusion protocol, volume of distribution was measured in control, septic (FIP or LPS), and SDX-treated 10 to 11 week old male mice. Data are represented as mean ± S.E.M. (n = 9–10). *$P < 0.05$ versus control; #$P < 0.05$ versus FIP or LPS.

structural and functional restoration of glycocalyx. Mitigation of increased vascular permeability in septic animals could be mechanistically linked to the restoration of glycocalyx.

It has been previously demonstrated that glycocalyx of endothelial cells and erythrocytes is impaired in the in vitro flow system when one of the cellular components has lost glycocalyx integrity (Oberleithner, 2013). The data on glycocalyx in neutrophils extend the previous observation: its integrity is lost in septic mice, and similar to the findings in endothelial cells SDX facilitates restoration of glycocalyx. This finding may have far-reaching consequences. The possibility arises that damaged EG affects the glycocalyx of all circulating formed elements. The corollary of such a prediction would be the increased egress of leukocytes, as well as hemolysis and dysmorphic changes in erythrocytes. In fact, these phenomena are observed in severe sepsis.

One of the limitations of this study is that the actual plasma concentration was not measured, which can provide information regarding therapeutic dose and insight into the possible mechanism or presence of delayed action of the agent. According to a human pharmacokinetic study, plasma concentration of SDX reaches up to 20 mg/l after 100 mg intravenous injection, decreases to 1 mg/l within 4 hours, and gradually approaches the undetectable range after 18 hours (Coccheri and Mannello, 2014). Based on these results, it can be suggested that the plasma concentration of SDX after a large dose (40 mg/kg) of subcutaneous injection may be maintained higher than IC_{50} for heparanase inhibition 5 mg/l (Masola et al., 2012) for the duration of our experiments.

In conclusion, these studies confirm the protracted nature of EG disintegration in sepsis, the event which contributes to high

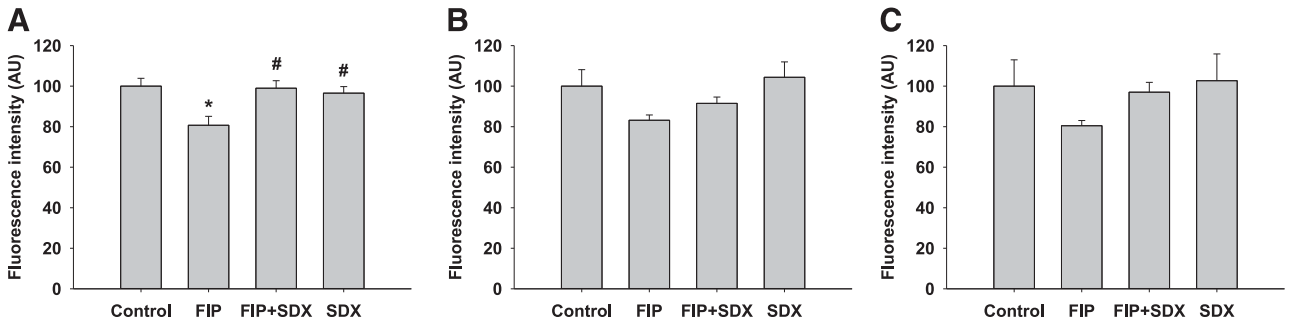

Fig. 7. Effect of treatments on aortic EG in mice. En face aortas were stained with WGA (A), antibodies against HS (B), and antibodies against syndecan 4 (C) in control and septic mice with or without SDX treatment. Statistically significant effect of SDX was documented for WGA staining (A), while HS and syndecan 4 (B and C) showed a trend toward improvement with SDX treatment. Data are represented as mean ± S.E.M. (n = 6). *$P < 0.05$ versus control; #$P < 0.05$ versus FIP.

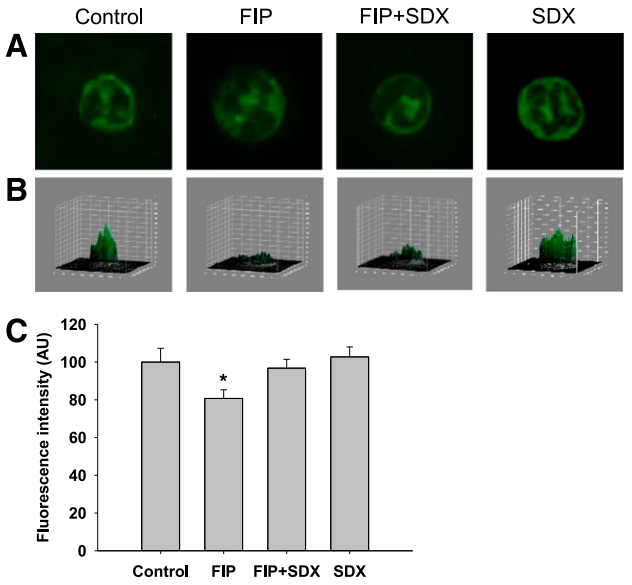

Fig. 8. Effect of SDX on neutrophil glycocalyx. Neutrophils were stained with WGA-lectin. (A) Representative images of stained neutrophils. (B) Three-dimensional plots of fluorescence intensity of neutrophils shown in (A). Note that the integrity of glycocalyx is impaired in FIP. (C) Summary of fluorescence intensity of 50 different cells per group. Data are represented as mean ± S.E.M. $^*P < 0.05$ versus control or FIP + SDX.

animal mortality. Restoration of disintegrated glycocalyx is accelerated in mice by administration of a heparin sulfate mimetic, SDX, which is resistant to heparanase. Finally, pharmacologic acceleration of EG restoration reduces vascular permeability, which is elevated in septic mice, and improves animal survival.

Acknowledgments

The authors are grateful to Dr. Yasuhiro Igarashi (Biotechnology Research Center, Toyama Prefectural University, Toyama, Japan) for kindly supplying hyaluromycin, which was used in the preliminary study.

Authorship Contributions

Participated in research design: Song, Zullo, Zhang, Goligorsky.
Conducted experiments: Song, Zullo, Liveris, Dragovich, Zhang.
Performed data analysis: Song, Zullo, Dragovich, Zhang.
Wrote or contributed to the writing of the manuscript: Song, Zullo, Dragovich, Zhang, Goligorsky.

References

Aird WC (2003) The role of the endothelium in severe sepsis and multiple organ dysfunction syndrome. *Blood* **101**:3765–3777.
Becker BF, Chappell D, Bruegger D, Annecke T, and Jacob M (2010a) Therapeutic strategies targeting the endothelial glycocalyx: acute deficits, but great potential. *Cardiovasc Res* **87**:300–310.
Becker BF, Chappell D, and Jacob M (2010b) Endothelial glycocalyx and coronary vascular permeability: the fringe benefit. *Basic Res Cardiol* **105**:687–701.
Becker BF, Jacob M, Leipert S, Salmon AH, and Chappell D (2015) Degradation of the endothelial glycocalyx in clinical settings: searching for the sheddases. *Br J Clin Pharmacol* **80**:389–402.
Chappell D, Heindl B, Jacob M, Annecke T, Chen C, Rehm M, Conzen P, and Becker BF (2011) Sevoflurane reduces leukocyte and platelet adhesion after ischemia-reperfusion by protecting the endothelial glycocalyx. *Anesthesiology* **115**:483–491.
Chelazzi C, Villa G, Mancinelli P, De Gaudio AR, and Adembri C (2015) Glycocalyx and sepsis-induced alterations in vascular permeability. *Crit Care* **19**:26.
Coccheri S and Mannello F (2014) Development and use of sulodexide in vascular diseases: implications for treatment. *Drug Des Devel Ther* **8**:49–65.
Dragovich MA, Chester D, Fu BM, Wu C, Xu Y, Goligorsky MS, and Zhang XF (2016) Mechanotransduction of the endothelial glycocalyx mediates nitric oxide production through activation of TRP channels. *Am J Physiol Cell Physiol* **311**: C846–C853.
Evanko SP, Tammi MI, Tammi RH, and Wight TN (2007) Hyaluronan-dependent pericellular matrix. *Adv Drug Deliv Rev* **59**:1351–1365.
Fraser JR, Laurent TC, and Laurent UB (1997) Hyaluronan: its nature, distribution, functions and turnover. *J Intern Med* **242**:27–33.
Ghosh CC, Mukherjee A, David S, Knaus UG, Stearns-Kurosawa DJ, Kurosawa S, and Parikh SM (2012) Impaired function of the Tie-2 receptor contributes to vascular leakage and lethality in anthrax. *Proc Natl Acad Sci USA* **109**:10024–10029.
Giantsos-Adams KM, Koo AJ, Song S, Sakai J, Sankaran J, Shin JH, Garcia-Cardena G, and Dewey CF, Jr (2013) Heparan sulfate regrowth profiles under laminar shear flow following enzymatic degradation. *Cell Mol Bioeng* **6**:160–174.
Guan H, Nagarkatti PS, and Nagarkatti M (2007) Blockade of hyaluronan inhibits IL-2-induced vascular leak syndrome and maintains effectiveness of IL-2 treatment for metastatic melanoma. *J Immunol* **179**:3715–3723.
Henry CB and Duling BR (1999) Permeation of the luminal capillary glycocalyx is determined by hyaluronan. *Am J Physiol* **277**:H508–H514.
Hoppensteadt DA and Fareed J (2014) Pharmacological profile of sulodexide. *Int Angiol* **33**:229–235.
Jiang D, Liang J, and Noble PW (2007) Hyaluronan in tissue injury and repair. *Annu Rev Cell Dev Biol* **23**:435–461.
Kaneider NC, Förster E, Mosheimer B, Sturn DH, and Wiedermann CJ (2003) Syndecan-4-dependent signaling in the inhibition of endotoxin-induced endothelial adherence of neutrophils by antithrombin. *Thromb Haemost* **90**:1150–1157.
Kusche-Vihrog K and Oberleithner H (2012) An emerging concept of vascular salt sensitivity. *F1000 Biol Rep* **4**:20.
Lipowsky HH, Sah R, and Lescanic A (2011) Relative roles of doxycycline and cation chelation in endothelial glycan shedding and adhesion of leukocytes. *Am J Physiol Heart Circ Physiol* **300**:H415–H422.
Mannello F, Medda V, Ligi D, and Raffetto JD (2013) Glycosaminoglycan sulodexide inhibition of MMP-9 gelatinase secretion and activity: possible pharmacological role against collagen degradation in vascular chronic diseases. *Curr Vasc Pharmacol* **11**:354–365.
Mannello F and Raffetto JD (2011) Matrix metalloproteinase activity and glycosaminoglycans in chronic venous disease: the linkage among cell biology, pathology and translational research. *Am J Transl Res* **3**:149–158.
Masola V, Onisto M, Zaza G, Lupo A, and Gambaro G (2012) A new mechanism of action of sulodexide in diabetic nephropathy: inhibits heparanase-1 and prevents FGF-2-induced renal epithelial-mesenchymal transition. *J Transl Med* **10**:213.
Morrison DC and Ulevitch RJ (1978) The effects of bacterial endotoxins on host mediation systems. A review. *Am J Pathol* **93**:526–618.
Nieuwdorp M, Mooij HL, Kroon J, Atasever B, Spaan JA, Ince C, Holleman F, Diamant M, Heine RJ, Hoekstra JB, et al. (2006a) Endothelial glycocalyx damage coincides with microalbuminuria in type 1 diabetes. *Diabetes* **55**:1127–1132.
Nieuwdorp M, van Haeften TW, Gouverneur MC, Mooij HL, van Lieshout MH, Levi M, Meijers JC, Holleman F, Hoekstra JB, Vink H, et al. (2006b) Loss of endothelial glycocalyx during acute hyperglycemia coincides with endothelial dysfunction and coagulation activation in vivo. *Diabetes* **55**:480–486.
Oberleithner H (2013) Vascular endothelium leaves fingerprints on the surface of erythrocytes. *Pflugers Arch* **465**:1451–1458.
Oberleithner H, Peters W, Kusche-Vihrog K, Korte S, Schillers H, Kliche K, and Oberleithner K (2011) Salt overload damages the glycocalyx sodium barrier of vascular endothelium. *Pflugers Arch* **462**:519–528.
Potter DR and Damiano ER (2008) The hydrodynamically relevant endothelial cell glycocalyx observed in vivo is absent in vitro. *Circ Res* **102**:770–776.
Ratliff BB, Rabadi MM, Vasko R, Yasuda K, and Goligorsky MS (2013) Messengers without borders: mediators of systemic inflammatory response in AKI. *J Am Soc Nephrol* **24**:529–536.
Reitsma S, Slaaf DW, Vink H, van Zandvoort MAMJ, and oude Egbrink MGA (2007) The endothelial glycocalyx: composition, functions, and visualization. *Pflugers Arch* **454**:345–359.
Spicer A and Calfee CS (2012) Fixing the leak: targeting the vascular endothelium in sepsis. *Crit Care* **16**:177.
van den Berg BM, Vink H, and Spaan JA (2003) The endothelial glycocalyx protects against myocardial edema. *Circ Res* **92**:592–594.
VanTeeffelen JW, Brands J, and Vink H (2010) Agonist-induced impairment of glycocalyx exclusion properties: contribution to coronary effects of adenosine. *Cardiovasc Res* **87**:311–319.
Vlasenko LP and Melendez AJ (2005) A critical role for sphingosine kinase in anaphylatoxin-induced neutropenia, peritonitis, and cytokine production in vivo. *J Immunol* **174**:6456–6461.
Vlodavsky I, Ilan N, Naggi A, and Casu B (2007) Heparanase: structure, biological functions, and inhibition by heparin-derived mimetics of heparan sulfate. *Curr Pharm Des* **13**:2057–2073.
Weinbaum S, Tarbell JM, and Damiano ER (2007) The structure and function of the endothelial glycocalyx layer. *Annu Rev Biomed Eng* **9**:121–167.
Wiesinger A, Peters W, Chappell D, Kentrup D, Reuter S, Pavenstädt H, Oberleithner H, and Kümpers P (2013) Nanomechanics of the endothelial glycocalyx in experimental sepsis. *PLoS One* **8**:e80905.
Zhang J, Skardal A, and Prestwich GD (2008) Engineered extracellular matrices with cleavable crosslinkers for cell expansion and easy cell recovery. *Biomaterials* **29**: 4521–4531.
Zullo JA (2016) *Mechanisms of Glycocalyx Loss at the Onset of Sepsis and Maneuvers for its Preservation and Regeneration* Ph.D. thesis, New York Medical College, Valhalla, NY.
Zullo JA, Fan J, Azar TT, Yen W, Zeng M, Chen J, Ratliff BB, Song J, Tarbell JM, Goligorsky MS, et al. (2016) Exocytosis of endothelial lysosome-related organelles hair-triggers a patchy loss of glycocalyx at the onset of sepsis. *Am J Pathol* **186**:248–258.

Address correspondence to: J.W. Song, Department of Anesthesiology and Pain Medicine, Yonsei University College of Medicine, 50 Yonsei-ro, Seodaemun-gu, Seoul, South Korea, 120-752. E-mail: sjw72331@yuhs.ac